Ensaios e Ciência
ISSN 1415-6938 e ISSN 2178-695X

DOI: https://doi.org/10.17921/1415-6938. 2026v30n3p371-383

Photodynamic Potential of Micellar Extracts of Spirulina and Chlorella by *Artemia Salina* Bioassay

Potencial Fotodinâmico de Extratos Micelares de Spirulina e Clorela Por Bioensaio Com Artemia Salina

Receveid: 05/12/2025
Accepted: 31/08/2026

Werlayne Vitalina Fontana Garcês : Universidade Estadual de Maringá, Departamento de Tecnologia. PR, Brazil.

João Gabriel Da Silva Andrade : Universidade Estadual de Maringá, Departamento de Engenharia Qúimica. PR, Brazil.

Carlos Eduardo Porto : Universidade Estadual de Maringá Departamento de Engenharia Quimica PR, Brazil.

Vanessa Daneluz Gonçalves : Universidade Estadual de Maringá, Departamento de Tecnologia. PR, Brazil.

Roberto Kenji Nakamura Cuman : Universidade Estadual de Maringá Departamento de Farmacologia e Terapêutica. PR, Brazil.

Vagner Roberto Batistela : Universidade Estadual de Maringá Departamento de Farmacologia e Terapêutica. PR, Brazil. E-mail: vrbatistela@uem.br

Abstract

Photodynamic inactivation generally utilizes synthetic photosensitizers of relatively high cost and difficult formulation, whose obtainment and final destination considerably impact the environment. Thus, the search for natural photosensitizers emerges as an alternative with greater sustainable viability. In this context, this study aimed to evaluate the photodynamic performance of micellar extracts of *Spirulina maxima* (SPI) and *Chlorella vulgaris* (CHLOR) formulated in the surfactant Pluronic® F-127, through toxicity bioassays with *Artemia salina*. The experiments were conducted in a photoreactor with a 50 W red LED lighting system, using a Box-Behnken experimental design to evaluate the factors: illumination time, dilution extraction factor, and NaCl concentration. Overall, the CHLOR extracts showed higher photodynamic activity than the SPI extracts. Furthermore, the illumination time was the most important factor in explaining the percentage of *A. salina* mortality. The extract dilution did not significantly affect *A. salina* mortality in the CHLOR assays, unlike what occurred with the SPI extracts, in which the 1/100 dilution promoted greater inactivation. The results show that CHLOR and SPI can offer promising sources of natural photosensitizers, favoring

therapeutic alternatives for photodynamic inactivation applications. These results pave the way for future studies, especially in the development of models to combat infections caused by pathogenic microorganisms, with the aim of expanding the treatment options available for human and animal health.

Keywords: Photodynamic Inactivation. Bioassay. Natural Photosensitizers.

Resumo

A inativação fotodinâmica geralmente utiliza fotossensibilizadores sintéticos de relatiovo alto custo e de difícil formulação, cuja obtenção e destino final impactam consideravelmente o meio ambiente. Assim, a busca por fotossensibilizadores naturais surge como uma alternativa com maior viabilidade sustentável. Neste contexto, este estudo teve como objetivo avaliar o desempenho fotodinâmico de extratos micelares de *Spirulina maxima* (SPI) e *Chlorella vulgaris* (CHLOR) formulados em surfactante Pluronic® F-127, por meio de bioensaios de toxicidade com *Artemia salina*. Os experimentos foram conduzidos em um fotorreator com sistema de iluminação LED vermelha de 50 W, utilizando um planejamento experimental Box-Behnken para avaliar os fatores: tempo de iluminação, fator de extração por diluição e concentração de NaCl. De forma geral, os extratos de CHLOR apresentaram maior atividade fotodinâmica do que os extratos de SPI. Além disso, o tempo de iluminação constituiu o fator mais importante para explicar a porcentagem de mortalidade de *A. salina*. A diluição do extrato não afetou significativamente a mortalidade de *A. salina* nos ensaios com CHLOR, ao contrário do que ocorreu com os extratos de SPI, nos quais a diluição de 1/100 promoveu maior inativação. Os resultados mostram que a CHLOR e SPI podem oferecer fontes promissoras de fotossensibilizadores naturais, favorecendo alternativas terapêuticas para aplicações de inativação fotodinâmica.Esses resultados abrem caminho para estudos futuros, especialmente no desenvolvimento de modelos para combater infecções causadas por microrganismos patogênicos, com o objetivo de ampliar as opções de tratamento disponíveis para a saúde humana e animal.

Palavras-chave: Inativação Fotodinâmica. Bioensaio. Fotossensibilizadores Naturais.

1 Introduction

The principle of photodynamic inactivation (PDI) relies on the interaction among three fundamental components: a photosensitizing compound, light at a specific excitation wavelength, and local molecular oxygen (Malá *et al*., 2021). This combination triggers a photochemical reaction that produces reactive oxygen species (ROS) (Correia *et al*., 2021; Youf *et al.,* 2021), imparting a bacteriostatic action with promising antimicrobial application (Garapati *et al*., 2023). The predominant mechanism involves the *in situ* generation of singlet oxygen, a highly cytotoxic species (Hamblin, 2016).

The quantum yield of singlet oxygen depends on the physicochemical characteristics of the photosensitizer and the medium (Buglak *et al*., 2021). Usually used in photodynamic activities, synthetic compounds include methylene blue, rose bengal, erythrosine, eosin, among others (Alasqah, 2024; Godard *et al*., 2020; Singh; Mukherjee, 2024). Alternatively, extracts derived from natural products represent a sustainable source of photosensitizers. Their viability stems from being relatively inexpensive, easy to obtain, and naturally rich in active ingredients (Muniyandi *et al*., 2020).

Extracts from *Spirulina maxima* (SPI) and *Chlorella vulgaris* (CHLOR) may offer promising

photosensitizers sources since their cellular structure contain dyes such as chlorophyll and cyano-phycocyanin that can absorb visible light (Abreu; Martins; Nunes, 2023; Correia *et al*., 2021; Rodrigues *et al*., 2024). Both SPI and CHLOR have certain characteristics that are necessary to photodynamically inactivate microorganisms, such as: easy access, economic viability, and pigments that absorb 600–800 nm wavelengths, favoring the penetration of light into tissues and providing excited states with sufficient energy to generate reactive oxygen species (Abrahamse; Hamblin, 2016).

In the search for new photosensitizers, few studies offer screening frameworks to evaluate photodynamic potential. Bioassays using *Artemia salina* nauplii are widely employed to evaluate substance toxicity and identify bioactive agents (Lourenço *et al*., 2022; Mota *et al*., 2024). This method has important features, such as quick results, easy setup, and low costs. The literature has successfully adapted this model to evaluate photodynamic activity, as for example in the studies of Pelossi *et al.* (2013) and Gerola *et al*. (2013).

Obtaining photoactive extracts of natural products with copolymeric surfactant offer better stability for the photosensitizers in solution, reducing their tendency to self-aggregate due to their incorporation into polymeric micelles (Vara *et al*., 2023). Photophysical studies have found that photosensitizer incorporated in micelles showed a long lifetime of singlet oxygen, increasing activity in photodynamic therapy (Mesquita *et al.,* 2018). These characteristics offer promising options to increase the performance of photodynamic processes (Turnovská; Etrych, 2025).

Despite the growing interest in natural photosensitizers, studies combining extracts of *Spirulina maxima* (SPI) and *Chlorella vulgaris* (CHLOR) in Pluronic® F-127 with *A. salina* bioassays remain unexplored. To address this gap, this study aimed to evaluate the photodynamic activity of SPI and CHLOR micellar extracts using *A. salina* nauplii as a rapid screening tool, coupled with multivariate analysis. A Box-Behnken design was applied to assess the effects of illumination time, extract concentration, and NaCl concentration to identify the conditions that maximize photodynamic mortality. Overall, this work provides a low-cost, effective strategy for screening microalgae-derived photosensitizers and highlights their potential for photodynamic applications.

2 Material and Methods

2.1 SPI and CHLOR extracts

To obtain the crude extract of SPI and CHLOR, 1,000 g of commercially purchased *Spirulina maxima* or *Chlorella vulgaris* (Wenutri Natural Foods & Supplements) were mixed with 10 mL of Pluronic® F-127 at 3.0% (w/v). The mixture was subjected to ultrasonic extraction for 15 min and then centrifuged for 5 min at 2,800 rpm. The micellar extract obtained after the separation of the centrifuged solid part was denominated as crude extract (CE). For subsequent assays, diluted extracts were obtained by 1/20, 1/50, and 1/100 dilution factors from the crude extract by addition of volumes

of 3.0% surfactant solution (w/v). The registration code on SISGEN is AFE292C.

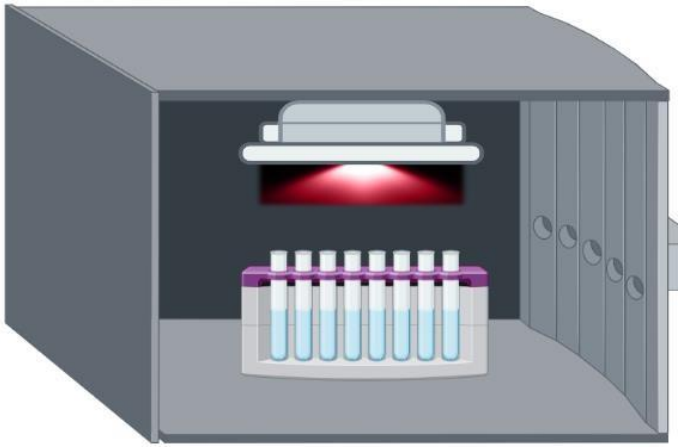
2.2 UV-Vis spectra

The UV-Vis absorption spectra of the SPI and CHLOR diluted extracts were obtained in a Shimadzu UV-1900 spectrophotometer with 1.0-cm optical path quartz cuvettes. The scan was performed in the range from 240 to 800 nm, with baseline correction.

2.3 Photoreactor and LED lighting system

A 33.0 cm × 33.0 cm × 29.5 cm photoreactor (Figure 1) was specifically developed to evaluate photodynamic activity *in vitro*. It is made of wood with a white coating that allows light to be reflected across the samples.

Figure 1 – Illustration of the photoreactor for photodynamic activity assays with *A. salina*



Source: the authors.

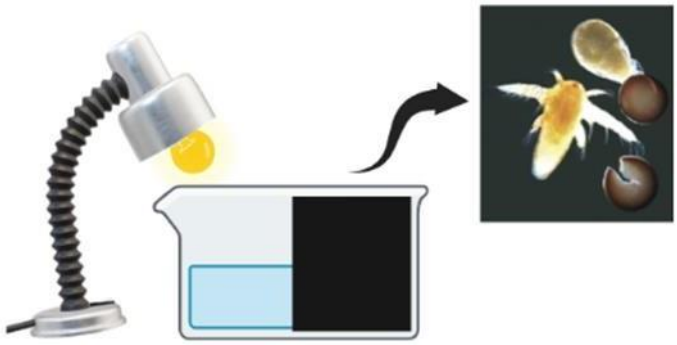
In its upper central portion, a mini LED (Light Emitting Diode) flood light reflector with 54 BRISA®, IP67, red 50-W connected red LED devices (irradiation in the red spectral region). In the photoreactor, the distance between the LED source and the surface of the liquids in the test tubes was 19 cm. This distance was kept constant in all experiments for comparison purposes as all experiments must emit the same the number of photons. LED offers an efficient, easy-to-acquire, and cheap alternative that yields excellent cost-benefit equipment for photodynamic applications (Sorbellini; Rucco; Rinaldi, 2018).

2.4 Photodynamic activity by bioassay

To evaluate photodynamic activity, *A. salina* nauplii were chosen since these microcrustaceans have greater sensitivity to light in their early stages of life (after 48 h of

hatching) (Munteanu; Dumitrascu, 2025). Initially, the hatching of *A. salina* cysts was carried out in a plastic container containing a dark region and a lighted region, which allows the nauplii to pass through as they hatch (Figure 2). The procedure was performed by adding a small amount of *A. salina* cysts to the dark portion, in a 0.10 mol/L NaCl solution. The system was illuminated for 48 h with a white light lamp at room temperature, until the hatching of the nauplii, which migrated from the dark to the light portion of the device.

Figure 2 – Hatching system of nauplii of *A. salina*



Source: the authors.

After hatching, about 20 nauplii were collected and added to test tubes with the aid of Pasteur pipettes. Then, 1.5 mL of SPI or CHLOR crude extract was diluted in 1/5, 1/10, 1/50, and 1/100 proportions and each test tube was filled with a saline solution (0.10 mol/L NaCl) up to 3.0 mL (the final volume). Then, the samples were irradiated with LED in the photoreactor, with distance of 19 cm between the LED and the surface of the liquid.

The mortality percentage was calculated by the ratio of the number of dead nauplii and the number of initial nauplii (Eq. 1). All experiments were performed in triplicates.

$$\%\ of\ mortality = \frac{number\ of\ dead\ A.Salina}{number\ of\ initial\ A.Salina} \times\ 100\% \quad (1)$$

To statistically describe the results, the mean values of mortality percentages, standard deviations (s), and the coefficient of variation (CV) were calculated.

2.5 Box-Behnken experimental design

The Box-Behnken design was used, considering the percentage of mortality of nauplii of *A. salina* as a response. The following factors were evaluated: dilution factor (DF; 1/100, 1/50, and CE); lighting time (LT; 0, 12, and 24 h); and salt concentration (SC, 0, 0.05, and 0.10

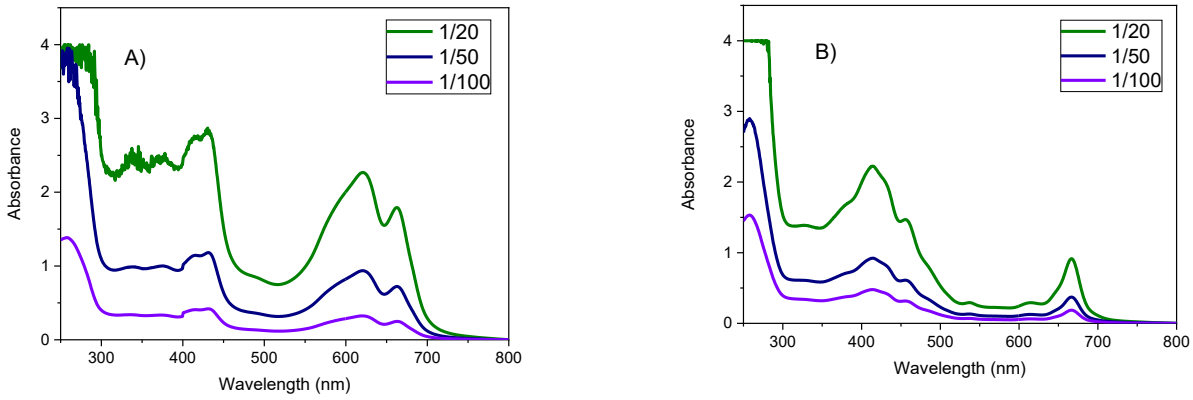
mol/L). The variation of each factor was coded as lower level (−1), central point (0), and upper levels (+1). Each group of experiments was analyzed in triplicates to determine their means, standard deviations, and coefficients of variation. Results were analyzed by analysis of variance (ANOVA) with $p<0.05$ for significance, and it was performed tests of relations between observed and predicted values, normal distribution of residuals, observed versus residual values, and residuals versus case number on Statistica® software, version 7.0.

3 Results and Discussion

3.1 UV-Vis spectra of SPI and CHLOR extracts

Figure 3A and 3B shows the UV-Vis absorption spectra of extracts at 1/20, 1/50, and 1/100 dilutions, for SPI and CHLOR respectively.

Figure 3 – Absorption spectra of the extracts at different dilutions. A) SPI; B) CHLOR



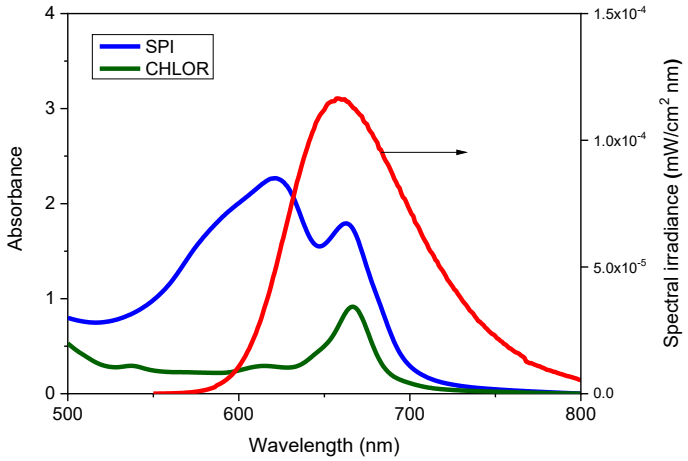
Source: the authors.

Bands at wavelengths around 420 nm possibly indicate the presence of carotenoids, and those in 620 nm and 660 nm to phycocynins and chlorine/chlorophyll, respectively (Afrasiabi *et al*., 2022). Chlorophyll is the most abundant dye in CHLOR and it can absorb light from 390 to 760 nm (Uliana *et al*., 2022).

SPI contains pigments such as c-phycocyanin and chlorophyll in its cellular structure, which give its bluish-green color and can comprise up to 75% of cyanobacteria such as SPI (Da Silva; Albuquerque; Becker, 2022) Both chlorophyll and phycocynins can absorb light at a maximum from 610 to 620 nm (Dranseikienė *et al*., 2022).

Figure 4 demonstrates the overlap between the absorption spectra of the extracts and the emission spectrum of the LEDs.

Figure 4 – Overlap of the emission spectrum of the red LED (red line) with the absorption spectra of the SPI (blue line) and CHLOR (green line) extracts at 1/20 dilutions



Source: the authors.

Based on Figure 4, it can be observed that both extracts show potential for photodynamic applications since the absorption region overlaps the emission region of the light source (Phasupan; Le; Nguyen, 2021). The absorption spectra of the extracts extend across the 600 to 800 nm range, known as the "phototherapeutic window". This wavelength range corresponds to red light emissions, which offer deeper light penetration into superficial tissues, such as the skin (Abrahamse; Hamblin, 2016).

3.2 Box-Behnken design

3.2.1 Main photodynamic parameters

Table 1 shows the Box-Behnken design to evaluate the influence of extract dilution, lighting time, and NaCl concentration on the mortality of the *A. salina*. In general, the highest mortality of *A. salina* was achieved with CHLOR extracts, which is indicative of the different compositions of the extracts of CHLOR and SPI, as shown by the UV-Vis spectra (Figure 3) and previously discussed.

Extracts of SPI and CHLOR showed that the conditions of assays 3 (1/100; 24; 0.05), 4 (CE; 24; 0.05), 10 (1/50; 24; 0), and 12 (1/50; 24; 0.10) yielded 100% of nauplii mortality. These results obtained the highest mortality percentages after 24 h of lighting once longer time irradiation favored the production of reactive oxygen species that promoted the mortality of *A. salina* (Overchuk *et al.,* 2023). These same results were found for the extracts of CHLOR, including assay 6 (CE; 12; 0).

Table 1 – Box-Behnken design of the mortality of *A. salina* with extracts of SPI and CHLOR, in relation to the dilution factor (DF), lighting time (LT) and salt concentration (SC)

Assay	DF	LT (h)	SC (mol /L)	SPI (%)	CHLOR (%)
1	1/100 (−1)	0 (−1)	0.05 (0)	40.69±0.54	24.73±0.32
2	CE (1)	0 (−1)	0.05 (0)	19.82±0.18	14.37±0.18
3	1/100 (−1)	24 (1)	0.05 (0)	**100.00±0.00**	**100.00±0.00**
4	CE (1)	24 (1)	0.05 (0)	**100.00±0.00**	**100.00±0.00**
5	1/100 (−1)	12 (0)	0 (−1)	67.25±0.35	98.45±2.69
6	CE (1)	12 (0)	0 (−1)	32.47±0.40	**100.00±0.00**
7	1/100 (−1)	12 (0)	0.10 (1)	70.31±0.19	88.55±0.58
8	CE (1)	12 (0)	0.10 (1)	35.35±0.15	86.55±0.85
9	1/50 (0)	0 (−1)	0 (−1)	26.00±0.53	30.79±0.76
10	1/50 (0)	24 (1)	0 (−1)	**100.00±0.00**	**100.00±0.00**
11	1/50 (0)	0 (−1)	0.10 (1)	33.03±0.46	39.13±0.82
12	1/50 (0)	24 (1)	0.10 (1)	**100.00±0.00**	**100.00±0.00**
13	1/50 (0)	12 (0)	0.05 (0)	45.03±0.50	92.42±0.10
14	1/50 (0)	12 (0)	0.05 (0)	44.70±0.44	93.87±0.88
15	1/50 (0)	12 (0)	0.05 (0)	45.05±0.31	91.21±1.52
16	1/50 (0)	12 (0)	0.05 (0)	45.27±0.43	93.32±1.67

Source: research data.

Both for SPI and CHLOR, the lowest mortality percentages occurred in assays 2 (CE, 0, 0.05), in which lighting duration equaled zero and crude extract. These percentages stemmed from the intrinsic action of the extract on the mortality of *A. salina*. The crude extract is higher in concentration of photosensitizers which can aggregate and difficult photodynamic action (Kazantzis et al., 2020).

Table 2 presents the analysis of variance (ANOVA) results for the mortality data of *A. salina* caused by SPI and CHLOR extracts.

Table 2 – ANOVA of *A. salina* mortality due to the photodynamic action of SPI and CHLOR extracts based in the Box-Behnken design

Extracts	Factor	SS	df	MS	F	p-value
SPI	DF (L+Q)	1071.2	2	535.6	9792.0	0.0001*
	LT (L+Q)	10956.4	2	5478.2	100151.9	0.0000*
	SC (L+Q)	56.6	2	28.3	517.3	0.0002*
	Error	420.4	9	70.1		
	Total SS	12504.6	15			
CHLOR	DF (L+Q)	63.9	2	31.9	23.7	0.0145*
	LT (L+Q)	14045.4	2	7022.7	5215.3	0.0001*
	SC (L+Q)	98.5	2	49.3	36.7	0.0078*
	Error	307.9	9	52.0		
	Total SS	14515.7	15			

Legend: SS = sum of squares; df = degrees of freedom; MS = mean square; F = calculated F value. * Significant values ($p<0.05$).
Source: research data.

From Table 2, the ANOVA of the SPI and CHLOR extracts revealed all the three variables were significant to explain photodynamic action of the extracts ($p<0.05$). The factor LT presents the greatest impact for the activity of both kind of extracts (higher F-values), demonstrating a strong

dependence of the photodynamic response on the irradiation intensity. This behavior suggests that increasing the illumination time intensifies the production of ROS, potentiating the phototoxic effect of the extract on the nauplii, as previously mentioned. In this way, Gerola *et al.* (2013) found that lighting duration constituted the most relevant factor in *A. salina* mortality. Bartolomeu *et al.* (2022) evaluated the photodynamic activity of isolated extracts of algae lipids irradiated with white light for the inhibition of *Staphylococcus aureus.* It observed that longer irradiation (90 min) completely inactivated the bacteria. However, the assay without exposure to light showed neither change nor antimicrobial activity.

The DF factor was found to be very important for SPI photodynamic action, once its SS value represents about ~9% of the total SS. The significant influence of DF factor also indicates that the concentration of photosensitizing compounds in the SPI directly affects the efficacy of the photodynamic process. For CHLOR, all variables proved to be significant, with LT also being identified as the most relevant among the three factors studied. For modeling the results, quadratic equations were proposed involving the three factors for SPI and CHLOR photodynamic activity, Eq. 2 and Eq. 3.

$$\%\text{mortality (SPI)} = 45.0 + 35.1*LT + 16.8*LT^2 - 11.3*DF + 3.4*DF^2 + 1.6*SC + 3.0*SC^2 \quad R^2 = 0.9664 \quad R^2\text{-adj}=0.9440 \tag{2}$$

$$\%\text{ mortality (CHLOR)} = 92.7 + 36.4*LT - 29.4*LT^2 - 1.4*DF - 3.5DF^2 - 1.9*SC + 4.2*SC^2 \quad R^2 = 0.9788 \quad R^2\text{-adj}=0.9646 \tag{3}$$

From the Eq. 2 and Eq. 3, the first value is the average of the % mortality for SPI and CHLOR, respectively, representative of the dataset in Table 1. It is noteworthy that the photodynamic action of CHLOR notably outperformed SPI, due to the higher amount of chlorophyll in its cellular structure, either due to better extraction efficiency, or due to the presence of more photosensitizers in the monomeric state. Once, chlorophylls are photosensitizers that can absorb red light, the more the monomeric photosensitizer absorbs light, the greater the photochemical reaction and generation of singlet oxygen (Gonçalves, 2021).

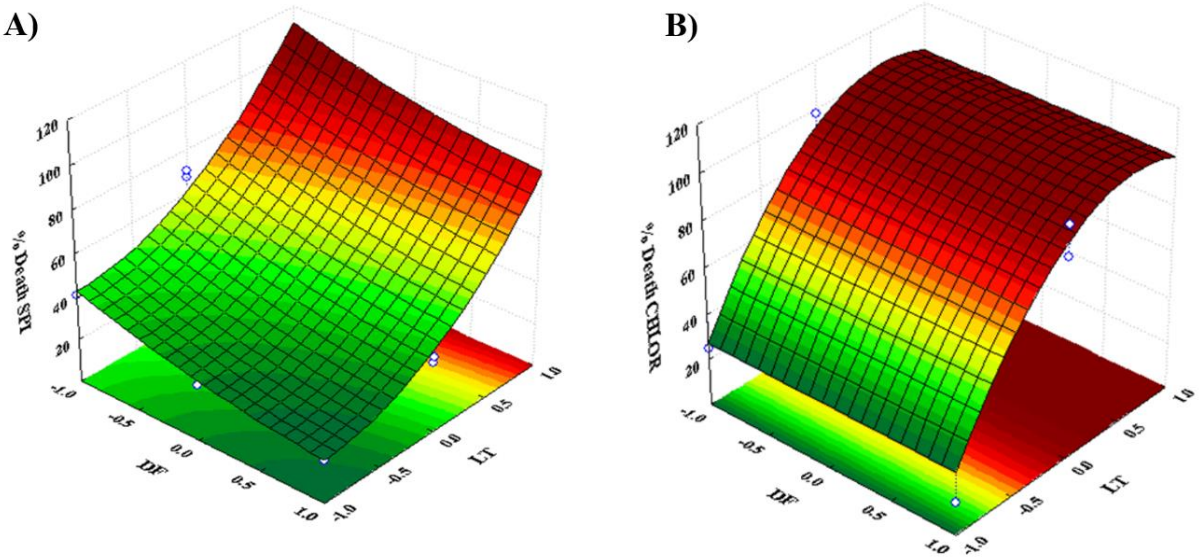
In Eq. 2 and Eq. 3, it is assessed that the quadratic model estimated for the percentage of mortality describes the highest coefficients for linear and quadratic LT, confirming the greater influence of this parameter on the response. The mathematical models were considered adequate because they involved all significant factors determined by ANOVA (Table 4) and by the high values of R^2 (> 0.96) and adjusted R^2 (> 0.94). The close proximity between the values of R^2 and adjusted R^2 adjusted in a regression model indicated that the independent variables (predictors) added to the model are relevant and not redundant in explaining the variation in the dependent variable (Haque *et*

al., 2020).

3.2.2 Response surface and mathematical models

Figure 6A represents the SPI response surface for mortality based on the second-order model described by Eq. 2. In this figure, it is shown 100% *A. salina* mortality at low dilution and long lighting time. Overall, the response surface suggests that longer lighting in higher dilutions promotes higher *A. salina* mortality.

Figure 6 – Response surfaces for *A. salina* mortality with lighting time and dilution factor as variables for A) SPI; B) CHLOR. The salt concentration was maintained at level -1 (no salt)



Source: the authors.

Both response surfaces showed curvature, especially due to the high coefficient value for the LT^2 factor, from both Eq. 2 and Eq. 3. In Figure 6A, the surface shows an upward trend, with the maximum mortality percentage at the minimum value (-1) for DF and at the maximum value (1) for LT. In Figure 6B, the region of maximum mortality percentage occurs at the maximum value (1) for LT, approximately independently of DF.

4 Conclusion

The bioassay with *Artemia salina* allowed the evaluation of the *in vitro* photodynamic action of different natural product extracts. Extracts of *Spirulina maxima* and *Chlorella vulgaris* with Pluronic® F-127 were effective in causing nauplii mortality under red LED light.

CHLOR extracts stood out as the most potent, promoting the highest mortality percentages of *A. salina.* The lighting time proved to be the most influential factor in photodynamic activity,

indicating that the photodynamic action depends on the production of ROS. An important consideration that affects photodynamic action is the dilution of the extract, so that the photosensitizers are in the monomeric state.

In this regard, these findings identify photodynamic conditions that warrant further biological assays—such as studies involving microorganisms or animals—to assess the potential for therapeutic application.

Acknowledgements
This study was financed in part by the Coordination for the Improvement of Higher Education Personnel – Brazil (CAPES) – Finance Code 001.

References

ABRAHAMSE, H.; HAMBLIN, M.R. New photosensitizers for photodynamic therapy. Bioch. J., v.473, n.4, p.347–364, 2016. doi: https://doi.org/10.1042/BJ20150942 .

ABREU, A.P.; MARTINS, R.; NUNES, J. Emerging applications of Chlorella sp. and Spirulina (Arthrospira) sp. Bioengineering, v.10, n.8, 2023. doi: https://doi.org/10.3390/bioengineering10080955 .

AFRASIABI, S. *et al*. The potential application of natural photosensitizers used in antimicrobial photodynamic therapy against oral infections. Pharmaceuticals, v.15, n.6, 2022. doi: https://doi.org/10.3390/ph15060767 .

ALASQAH, M. N. Efficacy of methylene blue-mediated antimicrobial photodynamic therapy on clinical and radiographic outcomes among patients with periodontal diseases: a systematic review and meta-analysis of randomized controlled trials. Photodiag. Photod. Ther., v.47, 2024. doi: https://doi.org/10.1016/j.pdpdt.2024.104000 .

BARTOLOMEU, M. *et al*. Bioprospecting antibiotic properties in photodynamic therapy of lipids from Codium tomemtosum and Chlorella vulgaris. Biochimie, v.203, p.32-39, 2022. doi: https://doi.org/10.1016/j.biochi.2022.09.012 .

BUGLAK, A.A. *et al.* Quantitative structure–property relationship modelling for the prediction of singlet oxygen generation by heavy-atom-free BODIPY photosensitizers. ChemRxiv, 2021. doi: https://doi.org/10.1002/chem.202100922

CORREIA, J.H. *et al.* Photodynamic therapy review: principles, photosensitizers, applications, and future directions. Pharmaceutics, v.13, n.9, 2021. doi: https://doi.org/10.3390/pharmaceutics13091332 .

DA SILVA, T.T.; ALBUQUERQUE, R.A.M.; BECKER, H. Ficocianina como indicador de cianobactérias em reservatórios. Quím. Nova, v.45, n.2, p.165-170, 2022. doi: https://doi.org/10.21577/0100-4042.20170814 .

DRANSEIKIENĖ, D. *et al.* Cyano-phycocyanin: mechanisms of action on human skin and future perspectives in medicine. Plants, v.11, n.9, 2022. doi: https://doi.org/10.3390/plants11091249

GARAPATI, C. *et al*. Photodynamic therapy: a special emphasis on nanocarrier-mediated delivery

of photosensitizers in antimicrobial therapy. Arab. J. Chem., v.16, n.4, 104516, 2023. doi: https://doi.org/10.1016/j.arabjc.2023.104583 .

GEROLA, A.P. *et al.* Estudos quimiométricos da pheo formulada em Pluronics®: ação fotodinâmica sobre Artemia salina. Química Nova doi: https://doi.org/10.1590/S0100-40422013000100018 .

GODARD, J. et al. New phenalenone derivatives: synthesis and evaluation of their singlet oxygen quantum yield. ACS Omega, v.5, n.43, p.28264–28272, 2020. doi: https://doi.org/10.1021/acsomega.0c04172 .

GONÇALVES, L.C.P. Photophysical properties and therapeutic use of natural photosensitizers. J. Photochem. Photobiol., v.7, p.1-15, 2021. doi: https://doi.org/10.1016/j.jpap.2021.100052

HAMBLIN, M. R. Antimicrobial photodynamic inactivation: a bright new technique to kill resistant microbes. Curr Opin Microbiol., v.33, p.67-73, 2016. doi: https://doi.org/10.1016/j.mib.2016.06.008

HAQUE, M.R. *et al.* Optimization of osmotic dehydration parameters of banana under pulsed microwave conditions by response surface methodology. J. Microbiol. Biotechnol. Food Sci., v.9, n.6, p.1053-1059, 2020. doi: 10.15414/jmbfs.2020.9.6.1053-1059 .

KAZANTZIS, K.T. *et al.* Curcumin derivatives as photosensitizers in photodynamic therapy: photophysical properties and in vitro studies with prostate cancer cells. Photoch. Photobiol. Sci., v.19, n.2, p.193-206, 2020. doi: https://doi.org/10.1039/C9PP00375D

LOURENÇO, Y.B.C. *et al.* Eucalyptus wood vinegar: chemical profiling, evaluation of acute toxicity to Artemia salina and effect on the hatching of Betta splendens eggs. Ensaios Ciênc., v. 25, n.5 (esp.), p.776-782, 2022. doi: https://doi.org/10.17921/1415-6938.2021v25n5-esp.p776-782

MALÁ, Z. et al. The application of antimicrobial photodynamic inactivation on methicillin-resistant S. aureus and ESBL-producing K. pneumoniae using porphyrin photosensitizer in combination with silver nanoparticles. Photodiag. Photod. Ther., v.33, 2021. doi: https://doi.org/10.1016/j.pdpdt.2020.102140 .

MESQUITA, M.Q. et al. An insight on the role of photosensitizer nanocarriers for photodynamic therapy. An. Acad. Bras. Ciênc., v.90, n.1, p.1101-1130, 2018. doi: https://doi.org/10.1590/0001-3765201720170800 .

MOTA, S.B.O. et al. Potencial larvicida de extratos de Stryphnodendron polyphyllum Mart. sobre Aedes aegypti e avaliação do efeito citotóxico e genotóxico. Ens. Ciênc., v.28, n.3, p.360-368, 2024. doi: https://doi.org/10.17921/1415-6938.2024v28n3p360-368

MUNIYANDI, K. *et al.* Role of photoactive phytocompounds in photodynamic therapy of cancer. Molecules, v. 25, n. 20, 4672, 2020. https://doi.org/10.3390/molecules25184102 .

MUNTEANU, C.; DUMITRASCU, M. Artemia salina. Disponível em: http://brineshrimp.wordpress.com/. Acesso em: 4 dez. 2025.

OVERCHUK, M. *et al.* Photodynamic and photothermal therapies: synergy opportunities for nanomedicine. ACS Nano, v.17, n.10, p.8562-8589, 2023. doi: 10.1021/acsnano.3c00891.

PELLOSI, D.S. et al. Evaluation of the photodynamic activity of xanthene dyes on Artemia salina described by chemometric approaches. Anais Acad. Bras. Ciênc., v.85, n.4, p.1267-1274, 2013. doi:

https://doi.org/10.1590/0001-3765201395412 .

PHASUPAN, P.; LE, T.D.; NGUYEN, L.T. Assessing the photodynamic efficacy of different photosensitizer–light treatments against foodborne bacteria based on the number of absorbed photons. J. Photochem. Photobiol. B: Biol., v.221, 2021. doi: 10.1016/j.jphotobiol.2021.112249.

RODRIGUES, A.C. *et al.* Photoinactivation of microorganisms using bacteriochlorins as photosensitizers. Braz. J. Microbiol., v.55, n.2, p.1139-1150, 2024. doi: https://doi.org/10.1007/s42770-024-01278-1 .

SINGH, S.; MUKHERJEE, T. K. Photosensitizer-free singlet oxygen generation via a charge transfer transition involving molecular O2 toward highly efficient oxidative coupling of arylamines to azoaromatics. Chem. Sci., v.15, n.34, p.13949-13957, 2024. doi: https://doi.org/10.1039/d4sc04115a .

SORBELLINI, E.; RUCCO, M.; RINALDI, F. Photodynamic and photobiological effects of light-emitting diode (LED) therapy in dermatological disease: an update. Lasers Med. Sci., v.33, n.7, p.1431-1439, 2018. doi: https://doi.org/10.1007/s10103-018-2584-8 .

TURNOVSKÁ, A.; ETRYCH, T. Polymeric micelles in advanced photodynamic therapy: design, delivery and translational prospects. Int. J. Pharm., v.7, 2025. doi: https://doi.org/10.1016/j.ijpx.2025.100439 .

ULIANA, M. P. *et al.* Photodynamic inactivation of microorganisms using semisynthetic chlorophyll a derivatives as photosensitizers. Molecules, v.27, n.18, 2022. doi: https://doi.org/10.3390/molecules27185769 .

VARA, J. *et al.* Polymeric micelles as a strategy to enhance the phototoxic efficacy of phenazine photosensitizers. Pol. Adv. Technol., v.34, n.11, p.3397-3406, 2023. doi: https://doi.org/10.1002/pat.6155 .

YOUF, R. *et al.* Antimicrobial photodynamic therapy: latest developments with a focus on combinatory strategies. Pharmaceutics, v.13, n.12, 1995, 2021. doi: https://doi.org/10.3390/pharmaceutics13121995 .